59^{th} *ILMENAU SCIENTIFIC COLLOQUIUM*
Technische Universität Ilmenau, 11 – 15 September 2017
URN: urn:nbn:de:gbv:ilm1-2017iwk-001:5

CONTOUR-INDEPENDENT DESIGN EQUATIONS FOR THE CALCULATION OF THE ROTATIONAL PROPERTIES OF COMMONLY USED AND POLYNOMIAL FLEXURE HINGES

Sebastian Linß[1], Philipp Schorr[2], Stefan Henning[1], Lena Zentner[1]

[1]Compliant Systems Group, Technische Universität Ilmenau
[2]Technical Mechanics Group, Technische Universität Ilmenau

ABSTRACT

Flexure hinges are often used as revolute joints in high-precision compliant mechanism, but without simulations the accurate prediction of their contour-dependent deformation and especially planar motion behavior is a challenging task. This paper presents contour-independent general design equations for the explicit calculation of the rotational stiffness, maximum angular deflection and rotational precision of various notch hinges in dependence of the geometric parameters. The non-linear analytical model describes a clamped beam with included flexure hinge which is loaded with a moment or a transverse force at its free end. In addition to the common semi-circular, corner-filleted, and elliptical flexure hinge, the high-performance polynomial hinge with five different orders is investigated. The deviation of the calculated results compared with the analytical solution depends on the contour and it is mostly relative low for the suggested parameter range. Furthermore, finite elements method (FEM) results correlate well with the predictions based on the analytical solution as well as the solution with the simple, concise and uniform design equations.

Index Terms - Compliant mechanism, Flexure hinge, Design equation, Polynomial contour

1. INTRODUCTION

In precision engineering applications and, in the course of technological progress, increasingly in micromechanical systems high standards for the drive and motion systems are necessary – especially regarding the precision and reproducibility. These requirements can be realized with conventional rigid-body mechanisms only with a great constructional effort or not at all. Because of their advantages, compliant mechanisms (e.g. [1], [2]) – often with concentrated distribution of compliance – have become established for these special guiding tasks. In monolithic mechanisms, the flexibility is achieved mostly by using notched flexure hinges (e.g. [3]), which replace the conventional revolute joints. But their motion is limited to small angular deflections of a few degrees because of their elastic deformation. The demand for a larger angular deflection and a low shift of the rotational axis results in a variety of sometimes very complex flexure hinge types, like the butterfly hinge [4] for example.

However, the investigations in this paper are focused on notch flexure hinges. Due to their low complexity they are easy to manufacture and therefore mainly used in plane compliant mechanisms, especially for kinematic chains with a higher link number. Furthermore, notch flexure hinges enable optimization potential regarding the rotational precision and possible deflection as equivalent objectives, which is not used yet. Mostly notch flexure hinges with basic cut-out geometries are used as material coherent joints realizing a plane rotation. Without simulations, their contour-dependent rotational properties are currently difficult to predict. Thus, simple and concise closed-form design equations for flexure hinges would be of great benefit to the accelerated and goal-oriented synthesis of compliant mechanisms.

This paper presents general design equations for the explicit calculation of the rotational stiffness, maximum angular elastic deflection and rotational precision of various notch flexure hinges in dependence of the geometric hinge parameters. The equations are derived for a moment and a transverse force loaded hinge by fitting the analytical results which are obtained due to modelling with the theory of large deflections of rods (non-linear Euler-Bernoulli theory). For the accurate model-based investigation of the rotational precision the fixed center approach is used to define the axis of rotation. Among the variety of existing notch geometries, four flexure hinge contours are selected and investigated: Three usual contours, the semi-circular, corner-filleted and elliptical contour, and as a novelty a polynomial contour with five different orders. Depending on the contour, the maximum root-mean-square error of the calculated results compared to the analytical solution is determined. Furthermore, FEM simulations are used to verify the equation-based predictions.

2. DESIGN OF THE FLEXURE HINGES

In contrast to form- and force-closed joints a flexure hinge enables a restoring force which can be advantageous in technical systems (this property is named *rotational stiffness*). According to the material coherent connection, the angular deflection of a flexure hinge is limited by reaching admissible material stress respective elastic strain values (*maximum angular deflection*). Thus, the motion range of a compliant mechanism is limited too – by the hinge in the kinematic chain with the largest rotation angle. In addition, no exact relative rotation is possible with a flexure hinge because always a shift of its axis of rotation occurs in dependence of geometric and load parameters (*rotational precision*). In turn, this can lead to path deviations of the compliant mechanism compared to the rigid-body mechanism, which are not negligible anymore, especially in precision engineering.

In the past, notch flexure hinges have been designed very frequently so that various cut-out geometries are proposed to describe the variable flexure hinge contour height $h_{\mathrm{n}}(x)$, see Fig. 1. Mostly, there are predefined basic geometry elements, which lead to three main notch flexure hinge types, each with a typical property: The precise hinge with a semi-circular contour [5], the large-deflective hinge with a corner-filleted contour [3] or the elliptical hinge [6] as a compromise. Furthermore, flexure hinges are designed with other elementary geometries to realize a special property, like the parabolic or hyperbolic contour [3], and cycloidal contour [7]. Increasingly flexure hinges are designed with a combination of the mentioned basic geometries [8]. Rarely special mathematical functions are used that allow more precise shape variations of the partial or whole hinge contour due to a higher number of geometric parameters, like the spline contour [9], the power-function contour [10], the exponent-sine contour [11], the Lamé contour [12], and the Bézier contour [13]. The design with undefined freeform geometries based on topology optimization [14] is a very complex, non-intuitive and not a general design process.

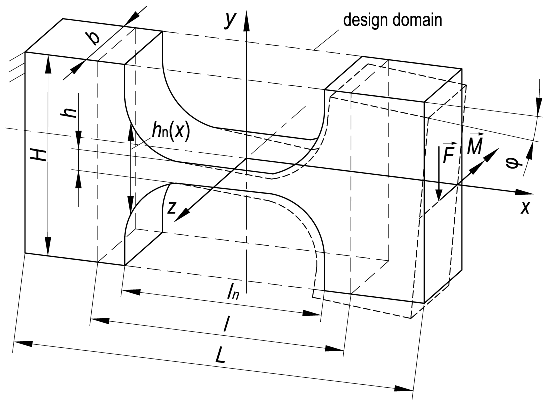

Fig. 1. Flexure hinge with geometric parameters and deflected state as a result of a moment or a force load

Nevertheless, higher order polynomial functions, which were suggested by the author in [15], are not state of the art. Among the variety of cut-out geometries especially polynomial contours offer high optimization potential whilst a comparatively simple contour modelling is possible. Depending on the polynomial order n and the coefficients arbitrary complex curves can be realized. Furthermore, nearly any elementary geometry could be approximated.

Subject of the investigations in this paper is a separate notch flexure hinge, which is fixed at one end (cf. Fig. 1). A given moment $\vec{M} = -M\vec{e}_z$ or transverse force $\vec{F} = -F\vec{e}_y$ leads to an plane angular deflection of the free end with the rotation angle φ. The variable hinge contour height $h_\mathrm{n}(x)$ is defined by the chosen notch geometry. As it is known, that a deformation not only occurs in the notch segment [16], the flexure hinge is always modelled with little segments of the both adjacent links.

Regarding the influence on the flexure hinge properties, two groups of geometric design parameters are investigated: The basic hinge dimensions (l, L, h, H, b) and the hinge contour (function $h_\mathrm{n}(x)$). A symmetric, continuously differentiable, not undercut hinge contour $h_\mathrm{n}(x)$ is regarded with the minimal notch height h in the middle (at $x = 0$), and with a rectangular cross-section. The total height H (which represents the link height in a compliant mechanism too) as well as the total length $L = 2H$ are chosen to be constant for all investigations. Thus, the distance of the acting load to the middle of the hinge is always half the length of L to ensure comparability. The hinge length l, the minimal hinge height h, and the hinge width b are varied within the design domain according to the introduced dimensionless ratios β_l, β_h, and β_b with

$$\beta_l = \frac{l}{H}\,,\ \beta_h = \frac{h}{H}\,,\ \text{and}\ \beta_b = \frac{b}{H}\,. \tag{1}$$

For the investigations in this paper four flexure hinge contours are considered (see Fig. 2), the three typical semi-circular, corner-filleted and elliptical contours, and a polynomial contour with five different orders. The latter represents a wide spectrum of different flexure hinges. Typical or – according to own investigations – suitable parameter values, like a stress optimal fillet radius [17], are already considered for the principle contour modelling.

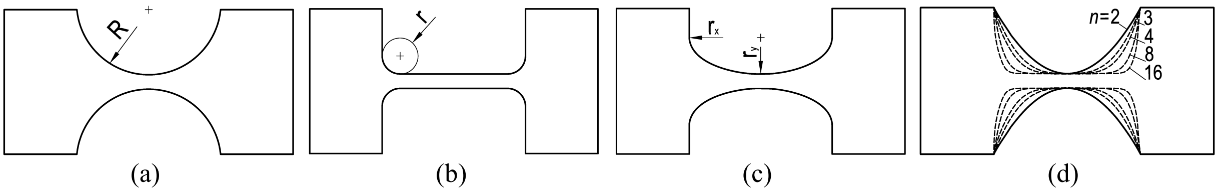

Fig. 2. Investigated notch contours with their basic parameters (shown for $\beta_l = 1$, $\beta_h = 0.1$): (a) semi-circular hinge with radius $R = 0.5l$; (b) corner-filleted hinge with stress optimal fillet radius $r = 0.1l$; (c) elliptical hinge with radii $r_x = 0.5l$ and $r_y = 0.25l$; (d) polynomial hinge with the orders *n* of 2, 3, 4, 8 and 16

Table 1. Used contour height functions for the four investigated flexure hinges

Hinge contour	$h_\mathrm{n}(x)$ and restrictions
Semi-circular	$h_\mathrm{n}(x) = h + 2R - 2\sqrt{R^2 - x^2}$; with $R = 0.5l$
Corner-filleted	$h_\mathrm{n}(x) = \begin{cases} h + 2r - 2\sqrt{r^2 - \left(x + \frac{l}{2} - r\right)^2}, & -\frac{l}{2} \le x < -\frac{l}{2} + r \\ h, & -\frac{l}{2} + r \le x \le \frac{l}{2} - r \\ h + 2r - 2\sqrt{r^2 - \left(x - \frac{l}{2} + r\right)^2}, & \frac{l}{2} - r < x \le \frac{l}{2} \end{cases}$; with $r = 0.1l$
Elliptical	$h_\mathrm{n}(x) = h + 2r_y\left(1 - \sqrt{1 - \frac{x^2}{{r_x}^2}}\right)$; with $r_x = 0.5l$ and $r_y = 0.25l$
Polynomial	$h_\mathrm{n}(x) = h + \frac{(H-h)}{\left(\frac{l}{2}\right)^n} x^n$

The four used hinge contour height functions $h_\mathrm{n}(x)$ are presented in Table 1. The exact notch length l_n depends on the notch contour and is mostly equal to the hinge length l. For more details regarding the exact CAD modelling see [18]. In case of the polynomial contours an odd polynomial order can also be achieved if the equation is used for a quarter hinge only, which has to be mirrored twice in the CAD model afterwards.

3. ANALYTICAL CHARACTERISATION

In this section, the non-linear analytical characterization of a notch flexure hinge is presented regarding its rotational stiffness, maximum angular elastic deflection, and rotational precision in dependence of the hinge contour and the geometric parameters β_l, β_h, and β_b. The analytical characterization is based on the non-linear theory for modelling large deflections of curved rods, e.g. [2], for which the dimensions of a cross-section are small compared to the rod length. Equilibrium equations are used to describe a rod element on the basis of the assumptions of a static problem for a slender structure with an axial inextensible line and the validity of Bernoulli hypothesis, Saint-Venant's principle, and Hooke's law.

Thus, for describing a flexure hinge four non-linear differential equations result:

$$\frac{\mathrm{d}M}{\mathrm{d}s} + F\cos\theta = 0, \tag{2}$$

$$\frac{\mathrm{d}\theta}{\mathrm{d}s} - \kappa = 0\text{ , with } \kappa = \frac{M}{E\,I_\zeta} \text{ and } I_\zeta = \frac{b\,{h_\mathrm{n}}^3}{12}, \tag{3}$$

$$\frac{\mathrm{d}u_\xi}{\mathrm{d}s} - \cos\theta + 1 = 0, \tag{4}$$

$$\frac{\mathrm{d}u_\eta}{\mathrm{d}s} - \sin\theta = 0. \tag{5}$$

The model considers a stationary coordinate system $\xi\ \eta\ \zeta$ with the origin O at the neutral axis at the fixed end of the flexure hinge, see Fig. 3. The parameter s describes the arc length of the neutral axis at the regarded cross-section point and it represents the coordinate of the axial beam line, which is equal to the ξ-axis only for the non-deflected hinge. At every point s of the beam, the curvature κ describes the gradient of the bending angle θ as a result of the given moment or force load. Due to the non-linear differential equation system, closed-form equations which describe the deflected state cannot be derived with reasonable effort. However, for the regarded hinge, which is fixed at one side and loaded at the free end, four boundary conditions and transformations can be applied for numerical solution:

$$\kappa(L) = \frac{M}{E\,I_\zeta}, \theta(0) = 0, u_\xi(0) = 0, u_\eta(0) = 0. \tag{6}$$

This boundary value problem is solved numerically with MATLAB by means of a classical four-step Runge-Kutta method which is implemented in the used *ode45* function (with a relative and absolute error tolerance value of 10^{-8}). Based on the calculated deflected state due to the applied load in point $P_2{}'$ both of the displacements u_ξ and u_η, and the bending angle θ can be determined for every point s, for example in point $P_1{}'$. Further, the bending angle $\theta(L)$ corresponds to the rotation angle φ of the hinge and it equals nearly exactly the bending angle in point $P_1{}'$ too.

The following analytical characterization for the rotational stiffness, strain, and rotational precision is exemplified for hard aluminum alloy EN AW 7075 with a Young's modulus of $E = 72$ GPa and Poisson's ratio of $\nu = 0.33$, which is widely used for precision engineering applications because of the high admissible elastic strain up to 0.5 %. As assumption a typical hinge height of $H = 10$ mm is chosen. According to this, the typical values of $\beta_l = 1$, $\beta_h = 0.03$, $\beta_b = 0.6$ are used for the geometric hinge parameters. The influence of these hinge parameters has been already described in [18].

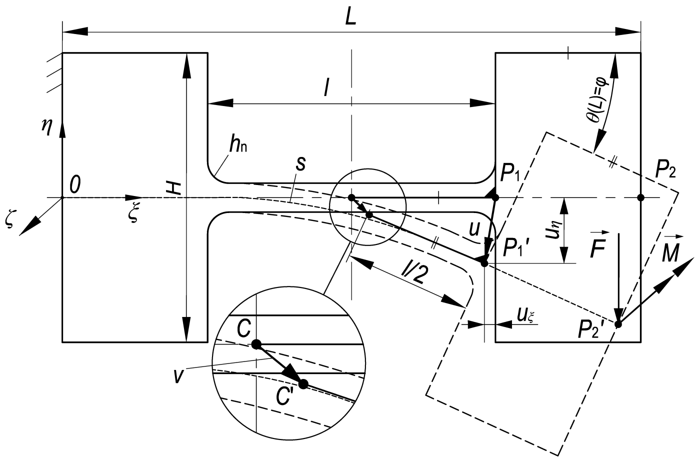

Fig. 3. Parameters of the flexure hinge in initial and deflected position with the model for the determination of the rotational axis shift based on guiding the center with a constant distance (fixed center approach)

3.1 Rotational stiffness

To evaluate the rotational stiffness, the $M(\varphi)$ respectively $F(\varphi)$ relation is considered in dependence of the load case. The influence of the hinge contour on the rotational stiffness is exemplarily shown in Fig. 4 for hinge dimensions, which are appropriate in precision engineering applications.

The principal load-angle-behavior is almost linear, which leads to a constant stiffness for the regarded small angular deflections up to 5°. The qualitative and quantitative correlation between the different hinge contours is similar for both loads. The following order can be generalized from the lowest to the highest stiffness: The corner-filleted, the 16th-order polynomial, the 8th-order polynomial, the 4th-order polynomial, the 3rd-order polynomial, the elliptical, the semi-circular and the quadratic polynomial contour. A flexure hinge with a quadratic polynomial contour is eight times stiffer than with a corner-filleted contour for this case of the regarded hinge dimensions.

3.2 Maximum strain and angular deflection

The bending stress is analyzed to characterize the maximum stress of the entire flexure hinge for a given deflection as a result of the moment or force load:

$$\sigma_{\mathrm{b}}(\xi)|_{\eta_{\max}} = \left|\frac{M_{\mathrm{b}}(\xi)}{w_{\mathrm{b}}(\xi)}\right| . \tag{7}$$

According to the theory, the maximum bending stress always results at the outer fiber for the maximum coordinate of η, which corresponds to the flexure hinge contour function. With the elastic section modulus for a rectangular cross-section and according to elastic deformation with a linear relation between stress and strain, the material independent strain is considered below. Thus, in dependence of the load case the contour-dependent strain is given by Eq. (8) for a moment load and by Eq. (9) for a transverse force load (with linearization).

$$\varepsilon(\xi) = \frac{6\,M}{E\,b\,h_{\mathrm{n}}(\xi)^2} \tag{8}$$

$$\varepsilon(\xi) = \frac{6\,(L-\xi)\,F}{E\,b\,h_{\mathrm{n}}(\xi)^2} \tag{9}$$

Taken into account a discrete deflection angle, we obtain the maximum strain $\varepsilon_{\max}$ at the outer fiber for the critical coordinate ξ_{crit} in dependence of the used contour function h_{n}, as shown in Fig. 5 for both load cases. The required input loads M and F are taken from Sect. 3.1. According to the theory, $\varepsilon_{\max}$ is independent of the width b for a given deflection.

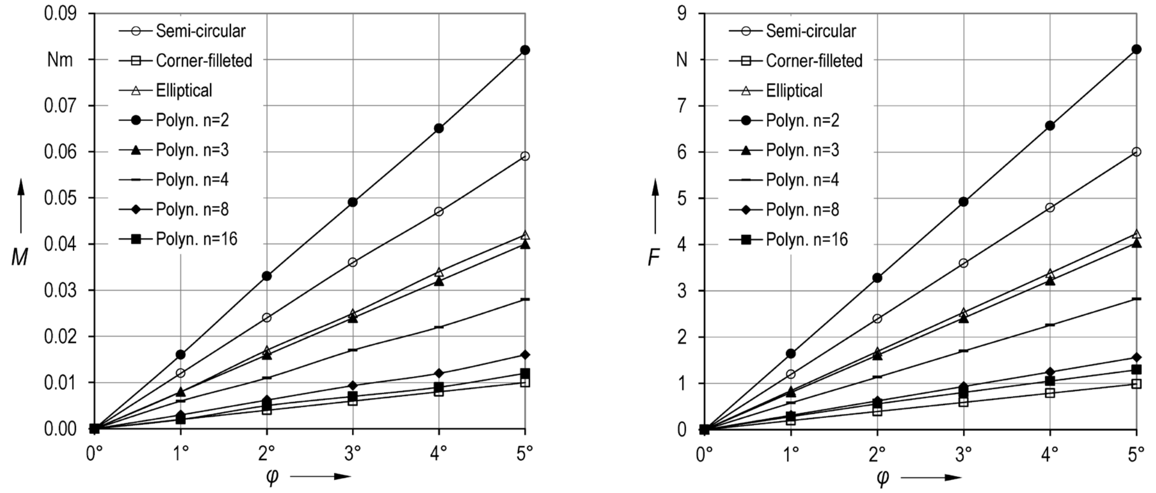

(a) (b)

Fig. 4. Analytical results for the rotational stiffness of a flexure hinge in dependence of the hinge contour ($\beta_l = 1, \beta_h = 0.03, \beta_b = 0.6$): (a) moment load, (b) force-load

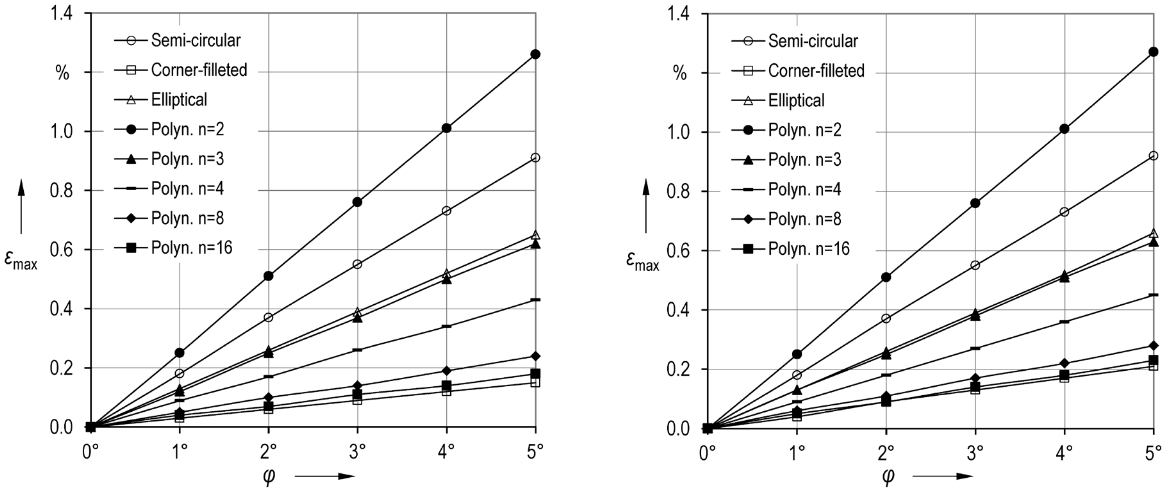

(a) (b)

Fig. 5. Analytical results for the maximum strain of a flexure hinge in dependence of the hinge contour ($\beta_l = 1, \beta_h = 0.03$): (a) moment load, (b) force-load

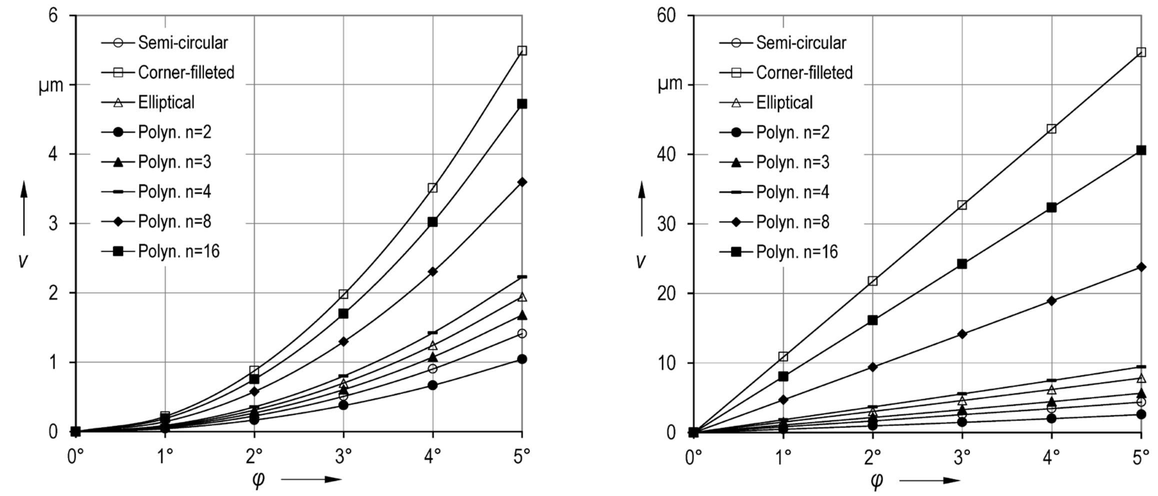

(a) (b)

Fig. 6. Analytical results for the rotational precision of a flexure hinge in dependence of the hinge contour ($\beta_l = 1, \beta_h = 0.03$): (a) moment load, (b) force-load

Among the regarded contours, the quadratic polynomial contour always leads to the highest strain values. In this case, the maximum admissible elastic strain of 0.5 % would be clearly exceeded for the aluminum material AW 7075. According to the following order – of using the semi-circular, the elliptical, the 3rd-order polynomial, the 4th-order polynomial, the 8th-order polynomial, the 16th-order polynomial, and the corner-filleted contour – the maximum strain value can be reduced. Some contours like the 16th-order polynomial, and the corner-filleted contour can be grouped as they show comparable properties.

The maximum strain value is almost independent of the load, while a force load leads to minimal higher values. Thus, mostly the deflection angle determines the resulting strain value. For a moment, $\varepsilon_{\max}$ occurs in the hinge center in general. In contrast to this, the critical coordinate ξ_{crit} of $\varepsilon_{\max}$ depends on the flexure hinge contour for a force load. While the maximum strain approximately occurs in the hinge center for semi-circular and elliptical contours too, the critical point ξ_{crit} moves in direction of the clamped hinge side the more the flexure hinge contour takes the form of a simple beam, e.g. the corner-filleted contour.

Furthermore, regarding a concrete application in a mechanism, the admissible elastic strain ε_{adm} of the material should be higher than the critical maximum strain of each flexure hinge:

$$\varepsilon_{\text{adm}} \geq \varepsilon(\xi_{\text{crit}}) = \frac{6\,M}{E\,b\,h_{\text{n}}(\xi_{\text{crit}})^2}\,, \tag{10}$$

$$\varepsilon_{\text{adm}} \geq \varepsilon(\xi_{\text{crit}}) = \frac{6\,(L-\xi_{\text{crit}})\,F}{E\,b\,h_{\text{n}}(\xi_{\text{crit}})^2}\,. \tag{11}$$

Hence, the contour-dependent correlation of the material-given admissible elastic strain ε_{adm} to the maximum allowable rotation angle $\varphi_{\max}$ is interesting. To obtain this correlation the load is stepwise increased and the critical strain is determined with MATLAB. Then, the maximum rotation angle can be calculated according to the numerical solution (cf. Sect. 4.2).

3.3 Rotational precision

In particular in precision engineering, the rotational precision of a flexure hinge is a very important performance criterion for the kinematic behavior of a compliant mechanism. The rotational axis shift v of a single flexure hinge (cf. Fig. 3) can influence the path deviation of a coupler point of the compliant mechanism. To evaluate the rotational precision, the rotational axis shift-angle relation $v(\varphi)$ is considered in dependence of the load case.

The rotational axis shift v has to be determined model-based. Therefore, the fixed center approach is suitable [17]. In this case, based on the hinge center point in the initial position, the absolute value of v equals:

$$v = \sqrt{\left(\xi_{C'} - \frac{L}{2}\right)^2 + \eta_{C'}{}^2} = \sqrt{\left(u_\xi - \frac{l}{2}\cos\varphi + \frac{l}{2}\right)^2 + \left(u_\eta - \frac{l}{2}\sin\varphi\right)^2}\,. \tag{12}$$

To determine the axis shift, the deformation u of one arbitrary point (e.g. point $P_1{}'$) at the free end and the rotation angle φ must be known only. The influence of the hinge contour on the rotational precision is shown in Fig. 6.

The axis shift-angle-behavior is non-linear for a moment load and almost linear for a force load for the regarded angle φ. Furthermore, the load case has a strong influence on the absolute value. Independent from the hinge contour, a transverse force leads to a significant larger axis shift than a moment for an equal φ. The hinge contour has a strong influence on the axis shift too. Regarding a high rotational precision respectively a small axis shift the following order can be generalized for thin hinges: The quadratic polynomial, semi-circular, 3rd-order polynomial, elliptical, 4th-order polynomial, 8th-order polynomial, 16th-order polynomial, and corner-filleted contour. A hinge with a quadratic polynomial contour can be over 20 times more precise than one with a corner-filleted contour (for a force load). But especially for short and thick hinges, this order could change – also for a mechanism [19].

4. CONTOUR-INDEPENDENT DESIGN EQUATIONS

Existing design equations from literature (e.g. [3], [20]-[22]) are characterized by a long expression and complex structural form. Further, they are mostly valid for a special group of flexure hinge contours only and they are not developed for all three rotational properties, regarded in this paper. Simple and concise analytically derived design equations, whose structural form is independent from the notch geometry, are not known to the authors.

The novel closed-form design equations for a flexure hinge with various notch contours are derived based on the analytical results (cf. Sect. 3) for a wide range of the three basic hinge dimensions of β_l, β_h and β_b. The considered moment or transverse force load acts close to the hinge center at $L = 2H = 20\,\mathrm{mm}$ (free end). A power function with two coefficients in dimensionless form is used, to consider the different properties. We have chosen the power function because its form is suitable to express the principle dependence of the basic geometric parameters, which is strictly monotonic increasing. Furthermore, the power function offers great shape variability with a minimal number of coefficients (cf. [18]).

4.1 Rotational stiffness

For a moment load the contour-independent design equation for the rotational stiffness of a flexure hinge results as (all parameters must be used in SI units/SI derived units)

$$\frac{M}{\varphi} = k_{M1}\, E\, \beta_b\, \beta_l^{(-k_{M2})} \beta_h^{(2+k_{M2})} H^3, \tag{13}$$

and taken into account a transverse force load we obtain the rotational stiffness as

$$\frac{F}{\varphi} = k_{F1}\, E\, \beta_b\, \beta_l^{(-k_{F2})} \beta_h^{(2+k_{F2})} H^2. \tag{14}$$

4.2 Maximum angular deflection

To obtain the design equations for the $\varphi_{\mathrm{max}}(\varepsilon_{\mathrm{adm}})$ correlation in dependence of the load case, the load M, represented in Eq. (13), and the load F, Eq. (14), are used in Eq. (10) and (11). Next, the critical location ξ_{crit} for the maximum strain at the outer fiber and the hinge height $h_{\mathrm{n}}(\xi_{\mathrm{crit}})$ for this location have to be considered in dependence of the load case.

According to the theory, for a moment load the maximum strain occurs contour-independent in the hinge center. Therefore, the critical hinge height $h_{\mathrm{n}}(\xi_{\mathrm{crit}})$ always equals the minimum hinge height h. If h is expressed by β_h, this leads to the following design equation for the maximum angular deflection due to a moment load:

$$|\varphi_{\mathrm{max}}| = \frac{\varepsilon_{\mathrm{adm}}}{6\, k_{M1}} \left(\frac{\beta_l}{\beta_h}\right)^{k_{M2}}. \tag{15}$$

For a transverse force load, the critical location depends on the hinge contour. For this reason, an additional dimensionless factor k_{crit} for the deviation to the hinge center is introduced in this case (see Table 2), and L is eliminated. It is assumed, that the maximum strain occurs approximately in the hinge center for a semi-circular and an elliptical contour, what leads to $k_{\mathrm{crit}} = 0.5$ for this cases. The factor for the corner-filleted contour with an optimal fillet radius can be expressed by β_l in general. Thus, in all three cases, the critical hinge height $h_{\mathrm{n}}(\xi_{\mathrm{crit}})$ equals the minimum hinge height h too. To determine the factor k_{crit} for the polynomial contours of different order, an additional power function with three constants was fitted with the function *fminsearch* in MATLAB, based on the calculated results for the locations ξ_{crit} over the whole parameter range. This leads to the following design equation for the maximum angular deflection due to a transverse force load:

$$|\varphi_{\mathrm{max}}| = \frac{\varepsilon_{\mathrm{adm}}}{12\,(1-k_{\mathrm{crit}})k_{F1}} \left(\frac{\beta_l}{\beta_h}\right)^{k_{F2}}. \tag{16}$$

Because the maximum strain value limits the deflection, the maximum rotation angle of a flexure hinge is always possible with a corner-filleted contour, while a quadratic polynomial contour leads to the lowest possible angles. Due to a higher maximum strain, the maximum angular deflection decreases for a force load, compared to a moment load, especially for larger angles. Depending on the load, the rotation angle of a corner-filleted contour is more than six times (moment) resp. four times (force) higher than of a contour with the highest strain values (cf. Table 3). Especially for flexure hinges made from plastic, with admissible strain values higher than 1 %, a large angular deflection can be realized in dependence of the chosen minimal height h.

4.3 Rotational precision

The design equations for the $v(\varphi)$ relation were developed based on the power function too. According to the analytical results (cf. Sect. 3.3) it is further assumed that v correlates with φ^2 for a moment load and with φ for a force load.

Thus, for a moment load the contour-independent design equation for the rotational precision of a flexure hinge results as:

$$\frac{v}{\varphi^2} = k_{vM1}\, \beta_l^{\,k_{vM2}}\, \beta_h^{\,(1-k_{vM2})} H, \tag{17}$$

and taken into account a transverse force load we obtain the rotational precision as

$$\frac{v}{\varphi} = k_{vF1}\, \beta_l^{\,k_{vF2}}\, \beta_h^{\,(2-k_{vF2})} H. \tag{18}$$

4.4 Contour-dependent coefficients

With the help of MATLAB the contour-specific coefficients of the power functions are determined based on a fitting procedure in order to realize the smallest maximum error over all calculated result points. The approach is explained in [18] in detail.

The resulting coefficients for all design equations are given in Table 2. The rounded coefficients (two digits) are determined for an appropriate parameter range for the dimensions β_l ($0.5 \le \beta_l \le 1.5$) and β_h ($0.03 \le \beta_h \le 0.1$). According to the theory, the accuracy of the results is independent of the parameter range for β_b. Depending on the contour, the relative root-mean-square error e_{rms} over all parameter combinations and coefficients is in the range of less than 2 % to less than 24 % compared to the analytical solution.

Table 2. Coefficients for design equations (13)-(18) in dependence of the flexure hinge contour, valid for appropriate hinge dimensions ($0.5 \le \beta_l \le 1.5$, $0.03 \le \beta_h \le 0.1$, β_b arbitrary) and an angular deflection $\varphi \le 5°$, with specification of the maximum root-mean-square error within the parameter range

Hinge contour	k_{M1} [10^{-3}]	k_{M2}	k_{F1} [10^{-2}]	k_{F2}	k_{crit}	k_{vM1} [10^{-3}]	k_{vM2}	k_{vF1} [10^{-2}]	k_{vF2}	e_{rms} [%]
Semi-circular	107.90	0.52	10.55	0.51	0.5	99.85	0.52	19.12	0.94	4.6
Corner-filleted	83.95	0.96	8.41	0.96	$0.5 - 0.2\,\beta_l$	85.76	0.95	9.20	1.89	2.1
Elliptical	82.50	0.54	8.27	0.54	0.5	114.35	0.57	18.21	1.14	2.5
2nd-ord. Polynomial	133.00	0.48	13.32	0.48	$0.4\,\beta_l^{(-0.005)}\beta_h^{(-0.075)}$	80.27	0.47	12.88	0.88	23.6
3rd-ord. Polynomial	120.23	0.65	12.04	0.65	$0.4\,\beta_l^{(-0.035)}\beta_h^{(-0.064)}$	72.25	0.64	6.67	1.29	21.6
4th-ord. Polynomial	112.07	0.74	11.22	0.74	$0.4\,\beta_l^{(-0.081)}\beta_h^{(-0.048)}$	71.32	0.73	6.24	1.47	16.4
8th-ord. Polynomial	98.24	0.87	9.84	0.87	$0.4\,\beta_l^{(-0.283)}\beta_h^{(-0.01)}$	74.00	0.87	6.59	1.73	9.2
16th-ord. Polynomial	90.82	0.93	9.10	0.93	$0.4\,\beta_l^{(-0.463)}\beta_h^{(-0.07)}$	77.63	0.93	7.25	1.87	3.9

5. FEM-BASED VERIFICATION AND COMPARISON OF RESULTS

For the FEM-based simulation of the flexure hinges ANSYS Workbench 17.1 is used. The CAD model and FEM model are shown in Fig. 7. The model includes an additional part which is fixed at the loaded hinge side to realize the direct determination of the rotational axis C according to the chosen fixed center approach (cf. Fig. 3). In the FEM model one end of the flexure hinge is fixed and the free end is stepwise loaded with a moment or transverse force load at the edge in point P_2. After determining the resulting rotation angle values with two points of the free end, the three performance criteria, the rotational stiffness $M(\varphi)$ respectively $F(\varphi)$, the rotational precision $v(\varphi)$ and the maximum strain $\varepsilon_{\max}(\varphi)$ are analysed in dependence of the hinge contour for typical geometric parameters. Additionally the maximum angular deflection $\varphi_{\max}$ is calculated for the given $\varepsilon_{\mathrm{adm}}$.

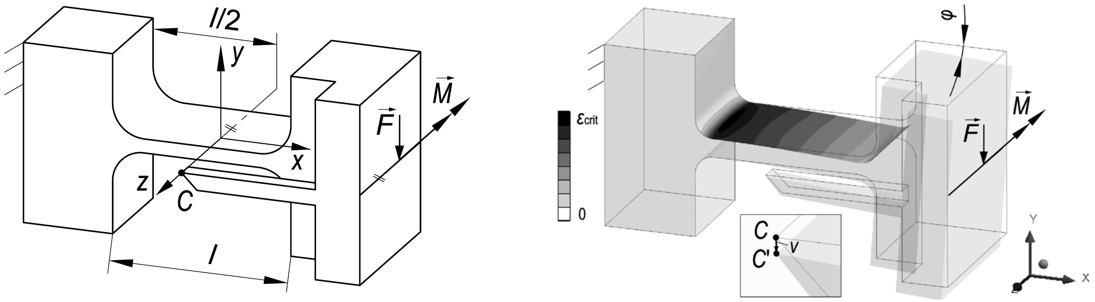

(a) (b)

Fig. 7. FEM-based characterization of a flexure hinge: (a) CAD model, (b) FEM model with initial and deformed hinge

According to the literature, the flexure hinge is modelled as a solid structure [23] with Solid186 hexahedral elements and with adjacent link segments [24], like they are considered for the analytical characterization too. In the FEM simulation large deflection is considered due to non-linear theory. Further assumptions are linear material behavior for the used aluminum AW 7075 material (with the same parameters like in Sect. 3) and a comparable fine discretization of all hinges.

The comparison of the analytical results, the design equation results and the FEM results for the eight investigated notch flexure hinges is shown in Table 3 for a moment and transverse force load for a discrete angular deflection. Additionally the relative deviations to the analytical solution are mentioned.

Generally, regarding all three performance criteria, the equation-based results and the FEM results are in good correlation with the analytical solution. Regarding all eight flexure hinges for the investigated hinge dimensions the minimum and maximum errors are 0 % resp. 14.7 % for the design equations and 0.1 % resp. 21.5 % for the FEM simulations. The differences, especially to the FEM results, can be explained with a more accurate modelling of a flexure hinge by means of FEM (e.g. consideration of shear stress and lateral contraction). But it must be considered, that the maximum relative errors always occur for very small absolute values, like for the rotational axis shift in the range of a few micrometers. Thus, the principle conclusions of Sect. 3 concerning the influence of the hinge contour on the rotational properties have been confirmed by different methods.

In conclusion, the suggested design equations are suitable to predict the deformation and motion behavior of a flexure hinge in dependence of the hinge contour within the investigated parameter range (cf. Table 2). The presented design equations are advantageous, because they are concise, and with only two coefficients their structural form is simple, contour-independent and – with the exception of the parameter H for geometric scaling – dimensionless. Taken into account a possible increasing error, the design equations could be applied for a larger range of the geometric parameters and rotation angle too.

Regarding the compliant mechanism application, the contour comparison confirms the potential of elliptical or 4th-order and to some extend 3rd-order polynomial contours to realize a large motion range with high precision. A strong influence of the contour on the flexure hinge properties exists in particular for thin hinges, which are suitable for application due to low strain values and thus larger angular deflections. Furthermore, the use of different flexure hinges in the same mechanism is promising especially in terms of variable higher order polynomial contours. In this case, the polynomial order can be adjusted easily in dependence of the relative rotation angle in the mechanism by using design graphs [25].

Table 3. Comparison of method-, contour- and load-dependent results for a discrete angular deflection $\varphi = 5°$ ($\beta_l = 1$, $\beta_h = 0.03$, $\beta_b = 0.6$) with specification of the relative errors to the analytical solution

Hinge contour	Method	Moment load				Force load			
		M [Nm]	v [µm]	$\varepsilon_{\max}$ [%]	$\varphi_{\max}$ [°]	F [N]	v [µm]	$\varepsilon_{\max}$ [%]	$\varphi_{\max}$ [°]
Semi-circular	a) analytical	0.0590	1.411	0.910	2.740	5.944	4.358	0.920	2.730
	b) design equation	0.0591	1.413	0.912	2.740	5.986	4.056	0.923	2.70
	deviation to a)	0.2 %	0.1 %	0.2 %	0.0 %	0.7 %	6.9 %	0.3 %	0.7 %
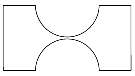	c) FEM	0.0622	1.428	0.892	2.803	6.240	5.020	0.894	2.796
	deviation to a)	5.4 %	1.2 %	2.0 %	2.3 %	5.0 %	15.2 %	2.8 %	2.4 %
Corner-filleted	a) analytical	0.0098	5.485	0.150	16.460	0.987	54.690	0.210	11.760
	b) design equation	0.0098	5.481	0.152	16.480	0.985	54.691	0.213	11.750
	deviation to a)	0.0 %	0.1 %	1.3 %	0.1 %	0.2 %	0.2 %	1.4 %	0.1 %
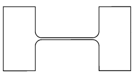	c) FEM	0.0102	5.367	0.166	15.060	1.025	54.720	0.228	10.965
	deviation to a)	4.1 %	2.2 %	10.7 %	8.5 %	3.9 %	0.1 %	8.6 %	6.8 %
Elliptical	a) analytical	0.0420	1.943	0.650	3.840	4.234	7.845	0.660	3.820
	b) design equation	0.0421	1.928	0.650	3.840	4.224	7.789	0.650	3.840
	deviation to a)	0.2 %	0.8 %	0.0 %	0.0 %	0.2 %	0.7 %	1.5 %	0.5 %
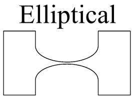	c) FEM	0.0446	1.906	0.641	3.900	4.481	8.551	0.639	3.912
	deviation to a)	6.2 %	1.9 %	1.4 %	1.6 %	5.8 %	9.0 %	3.2 %	2.4 %
2nd-ord. Polynomial	a) analytical	0.0820	1.042	1.260	1.980	8.217	2.585	1.270	1.980
	b) design equation	0.0840	0.943	1.295	1.930	8.396	2.214	1.244	2.010
	deviation to a)	2.4 %	8.5 %	2.8 %	2.5 %	2.2 %	14.4 %	2.0 %	1.5 %
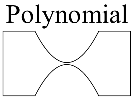	c) FEM	0.0852	1.138	1.368	1.827	8.555	3.140	1.369	1.826
	deviation to a)	3.9 %	9.2 %	8.6 %	7.7 %	4.1 %	21.5 %	7.8 %	7.8 %
3rd-ord. Polynomial	a) analytical	0.0400	1.680	0.620	4.030	4.037	5.657	0.630	3.960
	b) design equation	0.0420	1.557	0.644	3.880	4.181	4.828	0.644	3.880
	deviation to a)	5.0 %	7.3 %	3.9 %	3.7 %	3.6 %	14.7 %	2.2 %	2.0 %
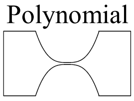	c) FEM	0.0427	1.758	0.694	3.602	4.285	6.242	0.694	3.602
	deviation to a)	6.8 %	4.6 %	11.9 %	10.6 %	6.1 %	10.3 %	10.2 %	9.0 %
4th-ord. Polynomial	a) analytical	0.0280	2.226	0.430	5.840	2.784	9.457	0.450	5.580
	b) design equation	0.0284	2.107	0.438	5.710	2.841	8.490	0.463	5.400
	deviation to a)	5.0 %	5.3 %	1.9 %	2.2 %	2.0 %	10.2 %	2.9 %	3.2 %
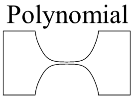	c) FEM	0.0294	2.190	0.414	6.039	2.946	9.980	0.439	5.695
	deviation to a)	6.8 %	1.6 %	3.7 %	3.4 %	5.8 %	5.5 %	2.4 %	2.1 %
8th-ord. Polynomial	a) analytical	0.0160	3.599	0.240	10.410	1.561	23.789	0.280	8.980
	b) design equation	0.0158	3.572	0.243	10.270	1.580	22.313	0.299	8.350
	deviation to a)	1.3 %	0.8 %	1.3 %	1.3 %	1.2 %	6.2 %	6.8 %	7.0 %
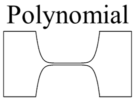	c) FEM	0.0164	3.651	0.270	9.259	1.643	24.180	0.298	8.389
	deviation to a)	2.5 %	1.4 %	12.5 %	11.1 %	5.3 %	1.9 %	6.4 %	6.6 %
16th-ord. Polynomial	a) analytical	0.0120	4.718	0.180	14.050	1.157	40.562	0.230	11.000
	b) design equation	0.0118	4.625	0.182	13.710	1.184	40.106	0.251	9.960
	deviation to a)	1.7 %	2.0 %	1.1 %	2.4 %	2.3 %	1.1 %	9.1 %	9.5 %
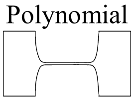	c) FEM	0.0119	4.731	0.198	12.658	1.207	40.738	0.236	10.593
	deviation to a)	0.8 %	0.3 %	9.7 %	9.9 %	4.3 %	0.4 %	2.6 %	3.7 %

6. CONCLUSIONS

In this paper, general design equations for the calculation of the rotational stiffness, maximum angular elastic deflection and rotational precision of various notch flexure hinges in dependence of the geometric hinge parameters are presented. The power function based closed-form equations are derived for a moment and a transverse force loaded hinge by fitting the analytical results which are obtained due to non-linear modelling with the theory of large deflections of rods. For the accurate model-based investigation of the rotational precision the fixed center approach is used to define the axis of rotation. Among the variety of existing notch geometries, four flexure hinge contours are selected and investigated: Three usual contours, the semi-circular, corner-filleted and elliptical contour, and the high-performance polynomial hinge contour with five different orders. Depending on the contour, the maximum root-mean-square error of the calculated results is in the range of less than 2 % to less than 24 % for an appropriate parameter range compared with the analytical solution. Furthermore, the FEM simulation results correlate well with the predictions based on the design equations. The equations are advantageous because with only two coefficients their structural form is simple, concise, contour-independent and dimensionless. Thus, the novel design equations contribute to the accelerated and goal-oriented synthesis of compliant mechanisms with the most commonly used hinge contours or the promising polynomial flexure hinges with an adjustable order. More hinge contours and other flexure hinge types could also be considered by determining the values of their coefficients in further research.

ACKNOWLEDGMENTS

The authors would like to gratefully acknowledge the support of the German Research Foundation (DFG) under Grant no. ZE 714/10-1.

REFERENCES

[1] Howell, L. L., Magleby, S. P., and Olsen, B. M.: Handbook of Compliant Mechanisms, Wiley, Chichester, 2013.

[2] Zentner, L.: Nachgiebige Mechanismen, De Gruyter Oldenbourg, München, 2014.

[3] Lobontiu, N.: Compliant Mechanisms: Design of Flexure Hinges, CRC Press, Boca Raton, Fla., 2003.

[4] Henein, S., Spanoudakis, P., Droz, S., Myklebust, L. I., and Onillon, E.: Flexure pivot for aerospace mechanisms, in: 10th European Space Mechanisms and Tribology Symposium, San Sebastian, Spain, 2003.

[5] Paros, J. M. and Weisbord, L.: How to design flexure hinges, Machine design, 25, 151–156, doi:10.1063/1.3137074, 1965.

[6] Smith, S. T., Badami, V. G., Dale, J. S., and Xu, Y.: Elliptical flexure hinges, Rev. Sci. Instrum., 68, 1474–1483, doi:10.1063/1.1147635, 1997.

[7] Tian, Y., Shirinzadeh, B., Zhang, D., and Zhong, Y.: Three flexure hinges for compliant mechanism designs based on dimensionless graph analysis, Precis. Eng., 34, 92–101, doi:10.1016/j.precisioneng.2009.03.004, 2010.

[8] Zelenika, S., Munteanu, M. G., and Bona, F. De: Optimized flexural hinge shapes for microsystems and high-precision applications, Mech. Mach. Theory, 44, 1826–1839, doi:10.1016/j.mechmachtheory.2009.03.007, 2009.

[9] Bona, F. De and Munteanu, M. G.: Optimized Flexural Hinges for Compliant Micromechanisms, Analog Integr Circ Sig Process, 44, 163–174, doi:10.1007/s10470-005-2597-7, 2005.

[10] Li, Q., Pan, C., and Xu, X.: Closed-form compliance equations for power-function-shaped flexure hinge based on unit-load method, Precis. Eng., 37, 135–145, doi:10.1016/j.precisioneng.2012.07.010, 2013.
[11] Wang, R., Zhou, X., and Zhu, Z.: Development of a novel sort of exponent-sine-shaped flexure hinges, Rev. Sci. Instrum., 84, 095008, doi:10.1063/1.4821940, 2013.
[12] Desrochers, S.: Optimum design of simplical uniaxial accelerometers, master thesis, McGill University, Montréal, 2008.
[13] Vallance, R. R., Haghighian, B., and Marsh, E. R.: A unified geometric model for designing elastic pivots, Precis. Eng., 32, 278–288, doi:10.1016/j.precisioneng.2007.10.001, 2008.
[14] Zhu, B. L., Zhang, X. M., and Fatikow, S.: Design of single-axis flexure hinges using continuum topology optimization method, Sci. China Technol. Sci., 57, 560–567, doi:10.1007/s11431-013-5446-4, 2014.
[15] Linß, S., Erbe, T., and Zentner, L.: On polynomial flexure hinges for increased deflection and an approach for simplified manufacturing, in: 13th World Congress in Mechanism and Machine Science, Guanajuato, Mexico, A11_512, available at: http://www.dmg-lib.org/dmglib/handler?docum=22411009, last access: 24 November 2016, 2011a.
[16] Zettl, B., Szyszkowski, W., and Zhang, W. J.: On Systematic Errors of Two-Dimensional Finite Element Modeling of Right Circular Planar Flexure Hinges, J. Mech. Des, 127, 782–787, doi:10.1115/1.1898341, 2005.
[17] Linß, S., Erbe, T., Theska, R., and Zentner, L.: The influence of asymmetric flexure hinges on the axis of rotation, in: 56th International Scientific Colloquium, Ilmenau, Germany, urn:nbn:de:gbv:ilm1-2011iwk-006:6, 2011.
[18] Linß, S., Schorr, P., and Zentner, L.: General design equations for the rotational stiffness, maximal angular deflection and rotational precision of various notch flexure hinges, Mech. Sci., 8, 29–49, doi:10.5194/ms-8-29-2017, 2017.
[19] Linß, S.: Ein Beitrag zur geometrischen Gestaltung und Optimierung prismatischer Festkörpergelenke in nachgiebigen Koppelmechanismen, doctoral thesis, TU Ilmenau, Ilmenau, urn:nbn:de:gbv:ilm1-2015000283, 2015.
[20] Paros, J. M. and Weisbord, L.: How to design flexure hinges, Machine design, 25, 151–156, doi:10.1063/1.3137074, 1965.
[21] Wu, Y. and Zhou, Z.: Design calculations for flexure hinges, Rev. Sci. Instrum., 73, 3101, doi:10.1063/1.1494855, 2002.
[22] Tseytlin, Y. M.: Notch flexure hinges: An effective theory, Rev. Sci. Instrum., 73, 3363–3368, doi:10.1063/1.1499761, 2002.
[23] Zhang, Z. and Hu, H.: Accurate Equivalent Beam Model of a Planar Compliant Mechanism with Elliptical Flexure Hinges, in: International Conference on Measuring Technology and Mechatronics Automation, Zhangjiajie, Hunan, China, 11–14, doi:10.1109/ICMTMA.2009.363, 2009.
[24] Yong, Y. K., Lu, T.-F., and Handley, D. C.: Review of circular flexure hinge design equations and derivation of empirical formulations, Precis. Eng., 32, 63–70, doi:10.1016/j.precisioneng.2007.05.002, 2008.
[25] Linß, S., Milojevic, A., Pavlovic, N. D., and Zentner, L.: Synthesis of Compliant Mechanisms based on Goal-Oriented Design Guidelines for Prismatic Flexure Hinges with Polynomial Contours, in: 14th World Congress in Mechanism and Machine Science, Taipei, Taiwan, doi:10.6567/IFToMM.14TH.WC.PS10.008, 2015.

CONTACTS

Dr.-Ing. S. Linß sebastian.linss@tu-ilmenau.de
M. Sc. P. Schorr philipp.schorr@tu-ilmenau.de
M. Sc. S. Henning stefan.henning@tu-ilmenau.de
Univ.-Prof. Dr.-Ing. habil. L. Zentner lena.zentner@tu-ilmenau.de